

Depth dependence of soil carbon temperature sensitivity across Tibetan permafrost regions

Jinquan Li^{a,b}, Dong Yan^a, Elise Pendall^b, Junmin Pei^a, Nam Jin Noh^b, Jin-Sheng He^{c,d}, Bo Li^a, Ming Nie^{a,*}, Changming Fang^{a,**}

^a Ministry of Education Key Laboratory for Biodiversity Science and Ecological Engineering, Coastal Ecosystems Research Station of the Yangtze River Estuary, Shanghai Institute of Eco-Chongming, Fudan University, 2005 Songhu Road, Shanghai 200438, China

^b Hawkesbury Institute for the Environment, Western Sydney University, Penrith 2751, NSW, Australia

^c Department of Ecology, College of Urban and Environmental Sciences, Key Laboratory for Earth Surface Processes of the Ministry of Education, Peking University, Beijing 100871, China

^d State Key Laboratory of Grassland and Agro-ecosystems, Lanzhou University, Lanzhou 730020, China

ARTICLE INFO

Keywords:

Permafrost
 Q_{10}
 Soil carbon decomposition
 Soil depth
 Structural equation model
 Tibetan Plateau

ABSTRACT

Permafrost regions with high soil organic carbon (SOC) storage are extremely vulnerable to global warming. However, our understanding of the temperature sensitivity of SOC decomposition in permafrost regions remains limited, leading to considerable uncertainties in predicting carbon-climate feedback magnitude and direction in these regions. Here, we investigate general patterns and underlying mechanisms of SOC decomposition rate and its temperature sensitivity (Q_{10}) at different soil depths across Tibetan permafrost regions. Soils were collected at two depths (0–10 and 20–30 cm) from 91 sites across Tibetan permafrost regions. SOC decomposition rate and Q_{10} value were estimated using a continuous-flow incubation system. We found that the SOC decomposition rate in the upper layer (0–10 cm) was significantly greater than that in the lower layer (20–30 cm). The SOC content governed spatial variations in decomposition rates in both soil layers. However, the Q_{10} value in the upper layer was significantly lower than that in the lower layer. Soil pH and SOC decomposability had the greatest predictive power for spatial variations in Q_{10} value within the upper and lower layers, respectively. Owing to the greater temperature sensitivity in the lower layer, our results imply that subsurface soil carbon is at high risk of loss, and that soil carbon sequestration potential might decrease in these regions in a warming world.

1. Introduction

Permafrost regions, where soil temperature remains below 0 °C for at least two consecutive years, are more vulnerable to climate change than other ecosystems (Schuur et al., 2008). These regions cover 23.6% of the total land area of the Northern Hemisphere, and are widely distributed across high-latitude and -altitude regions (Zhang et al., 2008b). Soil organic carbon (SOC) stored in permafrost regions is estimated at ~1024 Pg (1 Pg = 10¹⁵ g) for the 0–300 cm depth (Tarnocai et al., 2009), accounting for ~44% of the total global SOC stock (Jobbagy and Jackson, 2000). About 19% of the SOC in permafrost regions is stored at the 0–30 cm depth (Tarnocai et al., 2009). Over the last 30 years, the temperatures of high-latitude and -altitude regions have risen 0.6 °C per decade, twice as fast as the global average (IPCC, 2013), which may lead to the faster decomposition of SOC in these

regions (e.g., Schuur et al., 2015; Schädel et al., 2016). The corresponding release of carbon (C) could potentially drive one of the most significant feedback processes involving terrestrial ecosystems and atmospheric CO₂ concentrations (Davidson and Janssens, 2006).

The overall strength of soil C-climate feedbacks is unlikely to be effectively resolved by studies at individual sites, due to the high spatial heterogeneity (Zhou et al., 2009). Some studies have examined SOC decomposition rates and their temperature sensitivity (Q_{10}) in surface soils across large-scale permafrost ecosystems. For example, Ding et al. (2016a) found that precipitation governed spatial variation in SOC decomposition rate, while basal microbial respiration rate regulated Q_{10} values in surface soils of 0–10 cm across Tibetan permafrost regions. However, projecting future C cycling in permafrost is largely limited by uncertainties regarding the influence of soil depth on SOC decomposition rate and its temperature sensitivity. Because subsurface

* Corresponding author.

** Corresponding author.

E-mail addresses: mnjie@fudan.edu.cn (M. Nie), cmfang@fudan.edu.cn (C. Fang).

soils are projected to warm at roughly the same rate as surface soils over the next century (Hicks Pries et al., 2017), the dynamics of C that is sequestered at depth represent the most important source of uncertainty in projected future soil C dynamics (e.g., Koven et al., 2015; Balesdent et al., 2018). To the best of our knowledge, no previous studies have examined SOC decomposition rates and associated Q_{10} values for subsurface soils at a broad geographic scale in permafrost regions, which limits the ability to draw firm conclusions on the overall strength and geographical variability of C-climate feedbacks at different soil depths in permafrost regions.

Site-specific soil properties, such as soil nutrients (Rodionow et al., 2006), enzyme activities (Wang et al., 2013), microbial abundances (Waldrop et al., 2010), and microbial C accumulation efficiency (Jia et al., 2017) can lead to differing patterns of SOC decomposition and Q_{10} values in different soil layers. For instance, Waldrop et al. (2010) concluded that lower Q_{10} values in deeper soils relative to surface soils were attributable to lower microbial abundances and exoenzyme activities involved in subsoil SOC decomposition. However, Jia et al. (2017) found higher Q_{10} value in subsurface soil than in surface soil, possibly due to a higher proportion of resistant SOC in subsurface soil. Therefore, it is necessary to evaluate large-scale patterns and drivers of SOC decomposition rate and Q_{10} values in different soil depths in order to improve predictions of soil C-climate feedback magnitude and direction in permafrost regions.

The Tibetan Plateau is the highest and largest plateau on Earth, with a mean elevation of 4,000 m a.s.l. and area of $\sim 2.0 \times 10^6$ km² (Li and Zhou, 1998). Approximately three-quarters of the total area of alpine permafrost in the Northern Hemisphere is found on the Tibetan Plateau (Wang and French, 1995), making it the largest high-altitude permafrost region and a global hotspot for SOC storage (Mu et al., 2015), with one of the highest densities of SOC on the planet (Ding et al., 2016b). A recent study showed that the SOC pool in Tibetan permafrost is 15.31 Pg, 56% of which occurred in the top 1 m depth (Ding et al., 2016b). Unique geographical and climatic characteristics as well as the large SOC pool make the Tibetan Plateau ecosystem extremely sensitive to climate change. Similarly to other permafrost regions worldwide, the Tibetan Plateau has experienced significant warming (Wang et al., 2008), increased precipitation (Li et al., 2010), and permafrost thawing (Wu and Zhang, 2008) over recent decades. Furthermore, climate warming is projected to continue in the Tibetan Plateau in the future, with a temperature increase rate of about 0.3 °C per decade (Zhu et al., 2013). These trends, together with the highly complex temperature and moisture patterns (You et al., 2010), make the Tibetan Plateau an ideal ecosystem for continental-scale studies of variations in SOC decomposition rate and Q_{10} values with depth within permafrost regions.

This study represents the first large-scale exploration of the patterns and drivers of SOC decomposition rate and associated Q_{10} values with soil depth. We selected 91 sites across the Tibetan Plateau (Fig. 1), which were within the permafrost regions identified in a recent study by Ding et al. (2017). The mean active layer thickness is 2.4 m with a range of 1.3–3.5 m along the Tibetan Plateau (Pang et al., 2009), and soil samples in this study were collected from 0–10 and 20–30 cm depths. The aims of this study were to: 1) reveal patterns of SOC decomposition rate and its Q_{10} between the upper and lower layers across Tibetan permafrost regions; and 2) examine the relative importance of climatic drivers, biotic factors, and soil properties in regulating the spatial variations in SOC decomposition rate and Q_{10} in the two soil layers. Based on these aims, we proposed two initial hypotheses: 1) the SOC decomposition rate of the upper layer is greater than that of the lower layer, owing to higher C quality in the upper layer, whereas Q_{10} value is higher in the lower than in the upper layer, based on the C quality-temperature (CQT) hypothesis (Davidson and Janssens, 2006); 2) climatic and biotic factors play more important roles in the upper layer, whereas soil properties dominate in the lower layer for regulating spatial variations in SOC decomposition rate and Q_{10} value, because climate conditions more strongly affect the surface soil while factors

associated with C quality can be the determinant factors in subsurface soil.

2. Materials and methods

2.1. Study area and soil sampling

This study was conducted on the Tibetan Plateau, located in south-western China (Fig. 1). The climate is characterized as cold and dry across the main body of the Tibetan Plateau. The mean annual temperature (MAT) in this area ranges between -4.9 and 6.1 °C (Ding et al., 2016b), with the lowest mean monthly temperature in January and the highest in July (Chen et al., 2016); mean annual precipitation (MAP) varies from 84.3 to 593.9 mm, about 90% of which falls within the growing season from May to September (Ding et al., 2016b). The most representative vegetation types across Tibetan permafrost regions are alpine meadow and alpine steppe. More details of the study area can be found in Ding et al. (2016a).

Soil sampling was conducted along a 2,900 km-long, 800 km-wide transect of the central Tibetan Plateau. The transect spans latitudes $28^{\circ}12'–37^{\circ}30'$ N and longitudes $84^{\circ}06'–101^{\circ}12'$ E, and covers elevations from 2935 to 5420 m (Fig. 1b). During the summers (July and August) of 2012 and 2013, 91 sites (comprising 52 from the alpine meadow and 39 from the alpine steppe) were selected throughout the geographical extent of alpine grasslands on the Tibetan Plateau (Fig. 1b). A 100×100 m plot was set up at each site, and then five 1×1 m sub-plots were randomly set up within the 1 ha plot. After clipping the aboveground biomass in the five sub-plots, the upper (0–10 cm) and lower (20–30 cm) layer soils were sampled using a soil auger (diameter 7 cm). The soil was sampled from two separate layers, thereby decreasing the interactions between them. For instance, roots (belowground biomass, BGB) in the upper layer were approximately five-fold greater than in the lower layer (Fig. S1), suggesting that roots may have comparatively little effect on the lower layer. In each soil layer, two subsamples were collected within each 1×1 m sub-plot: one for soil analyses (soil incubation and soil properties) and the other for BGB analyses. In total, ten samples were collected from each layer at each site, with five for soil analysis and five for BGB estimation. Since our aim was to find a general pattern across broad geographical scales, not to assess within-site variability, the subsamples for soil and BGB analyses from each layer were each thoroughly homogenized and composited by depth. Plant roots in the homogenized sample were removed first by passing through a 2 mm mesh sieve and then by hand-picking the sieved samples until no visible roots were present. Approximately 50 g of soil was air dried and processed to determine its physical and chemical properties. The remaining soil was stored at 4 °C for incubation experiments.

2.2. Climatic variables and soil properties

Climate variables (MAT and MAP) at each site were derived from the WorldClim database (<http://www.worldclim.org>) in ESRI ARCMAP (ESRI 2011; Environmental Systems Research Institute, Redlands, CA, USA). To analyze soil properties, we selected three subplots from each plot for soil bulk density sampling, using a 100 cm^3 ring at each layer after clipping the aboveground biomass. Soil was oven dried for 48 h at 105 °C to calculate soil bulk density. The samples for BGB analyses were rinsed in a 0.15 mm screen mesh using deionized water, and then roots were oven-dried for more than one week to a constant weight at 65 °C. Soil pH was evaluated in deionized water solution (soil:solution = 1:2.5) using a pH meter (Seven-Compact S220, Mettler-Toledo AG, Switzerland). Soil total C (TC) and total nitrogen (TN) concentrations were determined using an elemental analyzer (PE 2400 II, Perkin-Elmer, Boston, MA, USA). Soil inorganic C (SIC) content was analyzed using an inorganic C analyzer (Calciometer 08.53, Eijkelkamp, Giesbeek, Netherlands) with HCl (4 mol L^{-1}) as titration solution (Chen et al.,

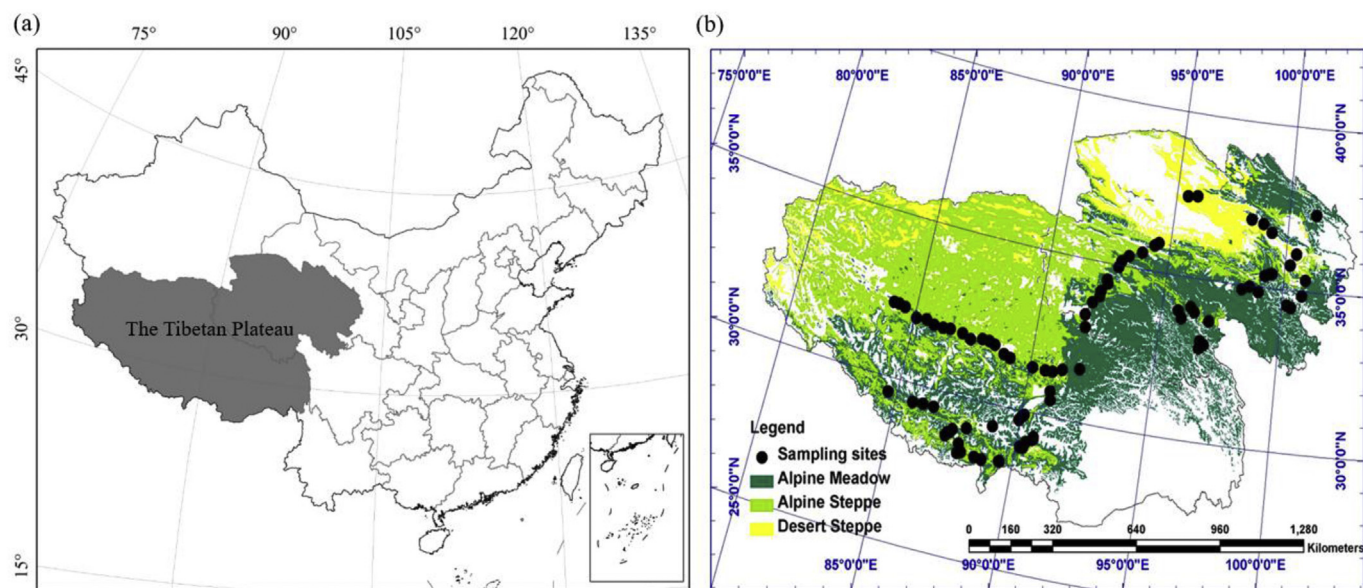


Fig. 1. Sampling sites and vegetation maps throughout the Tibetan Plateau. The vegetation map was obtained from China's vegetation atlas with a scale of 1:1,000,000 (Chinese Academy of Sciences, 2001).

2015). SOC was obtained as TC minus SIC. Soil water holding capacity (WHC) was gravimetrically determined on oven-dry soil.

2.3. Soil incubation and SOC decomposition rate measurements

Each fresh soil sample was divided into three experimental replicates (equivalent to 50 g dry weight) and incubated in 250 mL jars. All soils were adjusted to 60% WHC and pre-incubated at 20 °C for 72 h to avoid pulses in soil microbial activities induced by the disturbance of mixing and adjusting the soil moisture (Fierer et al., 2006). The SOC decomposition rate was then measured using a continuous-flow incubation system that we developed (see Fig. S2 for details).

In brief, the incubation temperatures ranged from 4 to 28 °C with a step of 4 °C in a water bath (± 0.05 °C) (DC0530; Bilanz Instrument Corp. Ltd., Shanghai). Temperature change of the water bath was automatically controlled by a linear uniform temperature change of 2 °C h^{-1} ; thus, a step of 4 °C temperature change took 2 h, which could minimize the influences of soil microbial activity by rapid temperature change. After each temperature change, an equilibration period of 2 h was required, and another 2 h was taken for decomposition rate measurement by a Picarro G2301 (Picarro, Inc., USA). Measurements were made using a continuous-flow incubation system with background gas (CO_2 concentration of 400 ppm) continuously passing the incubation jars at a flow rate of 50 scc min^{-1} (standard cubic centimeters per minute). This method minimized the inhibitory effects of high CO_2 concentrations on the SOC decomposition rate. During the incubation, the background gas was passed through deionized water before passing the incubation jars. Soil water loss was periodically checked gravimetrically and adjusted accordingly, with water loss not exceeding 2%. The purpose of this study was to reveal the potential sensitivity of SOC decomposition to temperature change, although the incubation temperature range in this study was greater than the actual temperature ranges for Tibetan permafrost regions. A similar incubation temperature range was previously used for estimating Q_{10} values in these regions (Ding et al., 2016a). No obvious inhibition of SOC decomposition was found across the temperature range (Fig. S3).

2.4. Calculations

The SOC decomposition rate calculation is found in the Supporting

Information. Eq. (1) was used to describe the relationship between the SOC decomposition rate and temperature (in this study, all fitting coefficients $R^2 > 0.95$; Fig. S3), and the Q_{10} value of SOC decomposition was calculated by Eq. (2) as below:

$$R = Be^{kT} \quad (1)$$

$$Q_{10} = e^{10k} \quad (2)$$

where R is the SOC decomposition rate ($\mu\text{g CO}_2\text{-C g}^{-1} \text{ soil h}^{-1}$), T is the incubation temperature (°C), and B and k are model fitting parameters.

Given the cold environment of the Tibetan Plateau, we used Eq. (3) to calculate the SOC decomposition rate at 5 °C (R_5) in order to compare the patterns and drivers of SOC decomposition rate in the upper and lower layers over a broad geographic scale. In addition, we used Eq. (4) to calculate the SOC decomposition rate per unit organic C at 5 °C, D_{soc} , to denote soil C decomposability; this is related to the availability and lability of C substrates. Parameter B from Eq. (1) is also widely used to represent C quality (e.g., Fierer et al., 2006; Ding et al., 2016a).

$$R_5 = Be^{5k} \quad (3)$$

$$D_{\text{soc}} = \frac{R_5}{\text{SOC}} \quad (4)$$

where R_5 is the SOC decomposition rate at 5 °C ($\mu\text{g CO}_2\text{-C g}^{-1} \text{ soil h}^{-1}$), B and k are model fitting parameters from Eq. (1), and D_{soc} is the decomposability of SOC at 5 °C ($\mu\text{g CO}_2\text{-C g}^{-1} \text{ SOC h}^{-1}$).

2.5. Statistical analyses

A paired samples t -test was applied to analyze the differences in R_5 or Q_{10} values between the upper and lower layers. Pearson correlation analyses were performed to show the relationships between R_5 or Q_{10} values and climatic factors, biotic factors, and soil properties. Statistical analyses and correlations were performed using IBM SPSS STATISTICS (version 22), and the curve fittings were performed using SIGMAPLOT (version 12.5).

Structural equation models (SEMs) were applied to quantify the direct and indirect factors regulating SOC decomposition rate and its temperature sensitivity in the upper and lower layers across Tibetan permafrost regions. In brief, we established a base model according to

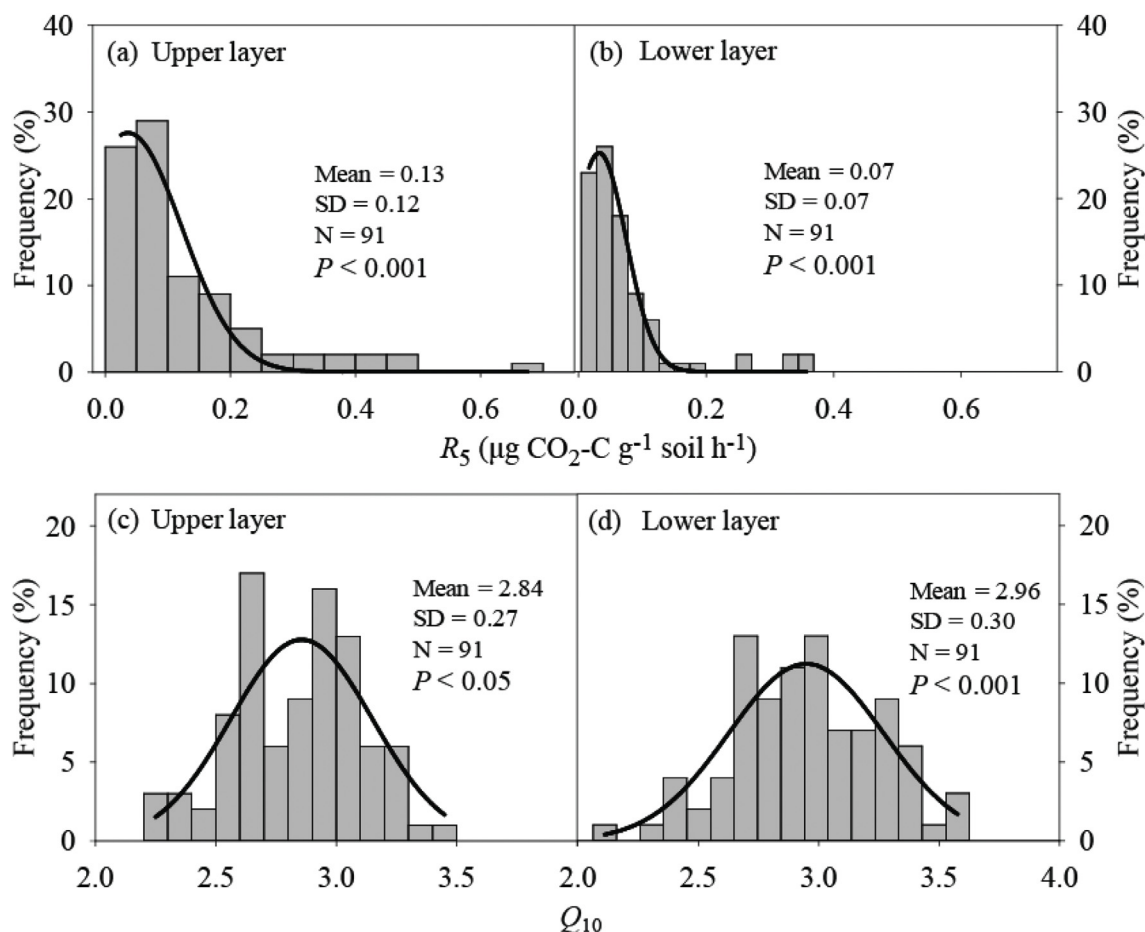


Fig. 2. Histogram plots of SOC decomposition rate at 5 °C (R_5) and Q_{10} value in the upper and lower layers across Tibetan permafrost regions. SD and N denote standard error and the sample size, respectively.

the correlation analyses between forcing variables and response variables (R_5 and Q_{10}) and empirical knowledge. We then optimized the base model according to the actual model fits, including the chi-square (χ^2) statistic, whole-model P value, goodness of fit index (GFI), and root-mean-square error of approximation (RMSEA). Data were fitted to the model using the maximum likelihood estimation method. SEM analyses were performed using AMOS 25 Graphics (IBM, SPSS, Armonk, NY, USA).

3. Results

3.1. SOC decomposition rates and Q_{10} values in the upper and lower layers

The SOC decomposition rate at 5 °C (R_5) exhibited large variations in both layers across Tibetan permafrost regions (Fig. 2), with a mean value of 0.13 $\mu\text{g CO}_2\text{-C g}^{-1}$ soil h^{-1} in the upper layer, which was significantly higher than that in the lower layer (0.07 $\mu\text{g CO}_2\text{-C g}^{-1}$ soil h^{-1}) ($P < 0.001$; Figs. 2 and S4). In addition, the R_5 values were higher at both depths in the alpine meadow than in the alpine steppe ($P < 0.05$; Fig. S4).

Large variations were also found in the Q_{10} values in both layers, ranging from 2.26 to 3.51 in the upper layer and 2.06 to 3.63 in the lower layer (Fig. 2). Across Tibetan permafrost regions, mean Q_{10} values in the upper soil layer were significantly lower than those in the lower soil layer (2.84 vs. 2.96, respectively; $P < 0.01$) (Figs. 2 and S5). The alpine steppe had higher Q_{10} values than the alpine meadow ($P < 0.05$), and the same depth pattern was noted in both subtypes (Figs. 2 and S5).

3.2. Correlations between R_5 or Q_{10} values and climatic factors, biotic factors, and soil properties

The SOC decomposition rate in the upper layer was significantly correlated with climatic factors (MAT and MAP), a biotic factor (BGB), and soil properties (bulk density, pH, SOC, and C:N ratio) ($P < 0.05$; Fig. 3). The same correlations were found in the lower layer, except that R_5 in the lower layer was not significantly correlated with the C:N ratio (Fig. 3). In both layers, R_5 was significantly positively correlated with MAP, BGB, and SOC, but negatively correlated with MAT, bulk density, and pH ($P < 0.05$; Fig. 3).

The Q_{10} values were significantly associated with a biotic factor (BGB) and soil properties (bulk density, pH, SOC, and C:N ratio) in the upper layer ($P < 0.05$; Fig. 4). However, in the lower layer, the Q_{10} values were significantly correlated with MAT, pH, SOC, and D_{soc} ($P < 0.05$; Fig. 4). Overall, the Q_{10} value in the upper layer was significantly and positively correlated with bulk density and pH, but significantly and negatively correlated with BGB, SOC, and C:N ratio ($P < 0.05$; Fig. 4); in the lower layer, the Q_{10} value was significantly and positively associated with MAT and pH, but negatively associated with SOC and D_{soc} ($P < 0.05$; Fig. 4).

3.3. Interacting factors influencing R_5 and Q_{10} in the upper and lower layers

The SOC decomposition rate at 5 °C (R_5) was mediated by different factors in the upper and lower layers (Fig. 5), explaining 26% and 50% of the spatial variation in R_5 values, respectively, across Tibetan permafrost regions (Fig. 5). Climatic factors played an important role only in the upper but not the lower layer (Fig. 5). In addition, SEM analyses

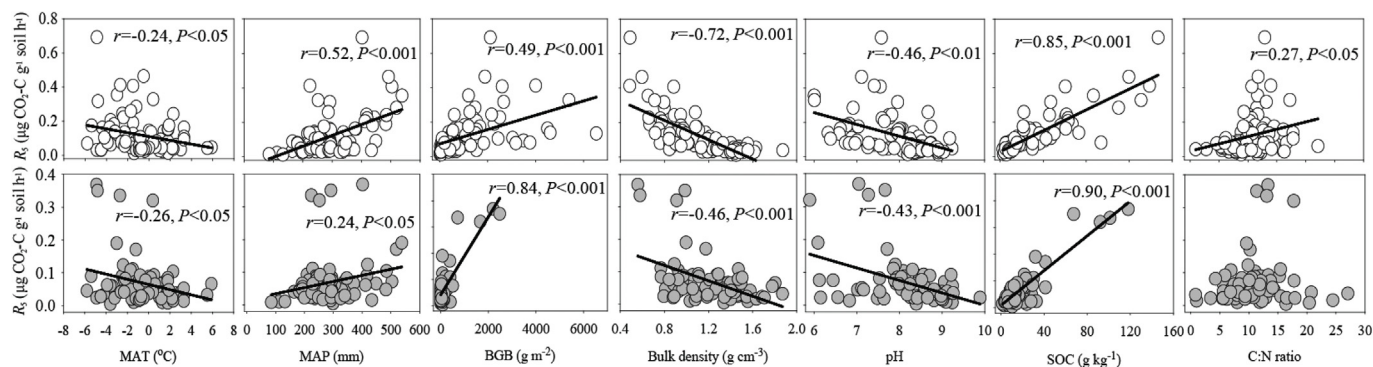


Fig. 3. Relationships of SOC decomposition rate at 5 °C (R_5) with climate factors (MAT, MAP), a biotic factor (BGB), and soil properties (bulk density, pH, SOC, and C:N ratio) across Tibetan permafrost regions. The white circles and grey circles denote the upper (0–10 cm) and lower (20–30 cm) layers, respectively. MAT, mean annual temperature; MAP, mean annual precipitation; BGB, below-ground biomass.

revealed that SOC had the greatest predictive power among the investigated variables for explaining the spatial variation in R_5 in both layers (Fig. 5).

Q_{10} values in the upper layer were influenced by a combination of biotic (BGB) and soil properties (SOC, pH, and C:N ratio), which together explained 72% of the spatial variation in Q_{10} across Tibetan permafrost regions (Fig. 6a). Only soil properties (pH, SOC, and D_{soc}) regulated the Q_{10} value in the lower layer, explaining 73% of the spatial variation (Fig. 6b). SEM analyses revealed that BGB and pH were the two main factors predicting Q_{10} values in the upper layer (Fig. 6c), while D_{soc} had the greatest power for predicting the spatial variation in Q_{10} values in the lower layer, followed by pH and SOC (Fig. 6d).

4. Discussion

Soils in permafrost regions store a large amount of C which is sensitive to climate change (Ding et al., 2016b); therefore, understanding SOC decomposition rates and their temperature sensitivity in these regions is crucial for predicting changes in global soil C stocks (Davidson and Janssens, 2006; Mu et al., 2015). Previous studies were mainly conducted at individual sites (e.g., Waldrop et al., 2010; Jia et al., 2017), whereas no attempts have been made to examine the patterns and drivers of SOC decomposition rates and Q_{10} values in different soil layers across a broad geographical scale in these regions, consequently adding considerable uncertainty to predictions of the magnitude and direction of C-climate feedbacks. This study is the first to demonstrate and investigate a general pattern of higher SOC decomposition rate, but lower Q_{10} values, in the upper than in the lower layer across Tibetan permafrost regions.

4.1. Depth dependence of SOC decomposition rates and Q_{10} values

The SOC decomposition rate was depth dependent due to the significant differences in SOC quantity and decomposability between the upper and lower layers. In this study, BGB was approximately five-fold greater in the upper than in the lower layer (Fig. S1), possibly leading to a higher C content in the upper relative to the lower layer (Liu et al., 2012). In addition, the higher decomposability of SOC in the upper layer may be attributed to less physical protection by soil minerals (Hassink and Whitmore, 1997), or the greater chemical availability of SOC for microbial metabolism (Bosatta and Ågren, 1999). Using a database of long-term (> 1 year) aerobic incubations of soils from permafrost regions, Schädel et al. (2014) also showed that the SOC pool and decomposability were higher in shallow than in deeper mineral soils.

Over a broad geographical scale, our study showed that Q_{10} values in the lower layer were significantly higher than in the upper layer across Tibetan permafrost regions (Fig. 2). Higher Q_{10} values in the lower layer could be mainly explained by the lower SOC decomposability in the lower layer. Enzymatic reactions of decomposing lower-quality SOC have higher activation energies and temperature dependence than reactions decomposing higher-quality SOC (Bosatta and Ågren, 1999; Davidson and Janssens, 2006). Therefore, the SOC decomposition in the lower layer should be inherently more temperature dependent than in the upper layer.

The annual net primary production on the Tibetan Plateau increased from 114.7 $\text{g C m}^{-2} \text{ yr}^{-1}$ in 1982 to 129.9 $\text{g C m}^{-2} \text{ yr}^{-1}$ in 2009 (Zhang et al., 2014), which might lead to an increase in plant C inputs to soil. Concordant with this speculation, a recent study by Ding et al. (2017) observed overall SOC accumulation rate of 28.0 $\text{g C m}^{-2} \text{ yr}^{-1}$ in the top 30 cm depth between the early 2000s and 2010s across Tibetan permafrost regions, and this accumulation was observed only in

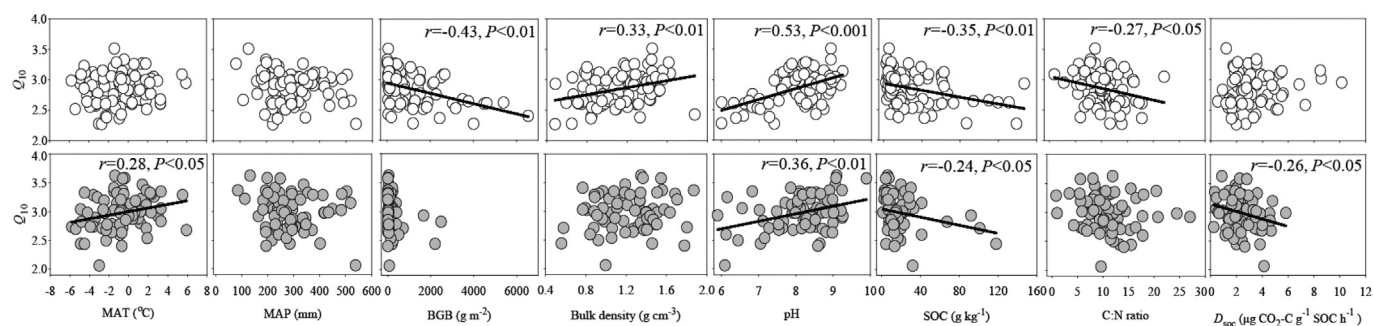


Fig. 4. Relationships of Q_{10} value with climate factors (MAT, MAP), biotic factor (BGB), and soil properties (bulk density, pH, SOC, C:N ratio, and D_{soc}) across Tibetan permafrost regions. The white circles and grey circles denote the upper (0–10 cm) and lower (20–30 cm) layers, respectively. MAT, mean annual temperature; MAP, mean annual precipitation; BGB, below-ground biomass; D_{soc} , SOC decomposability obtained from Eq. (4).

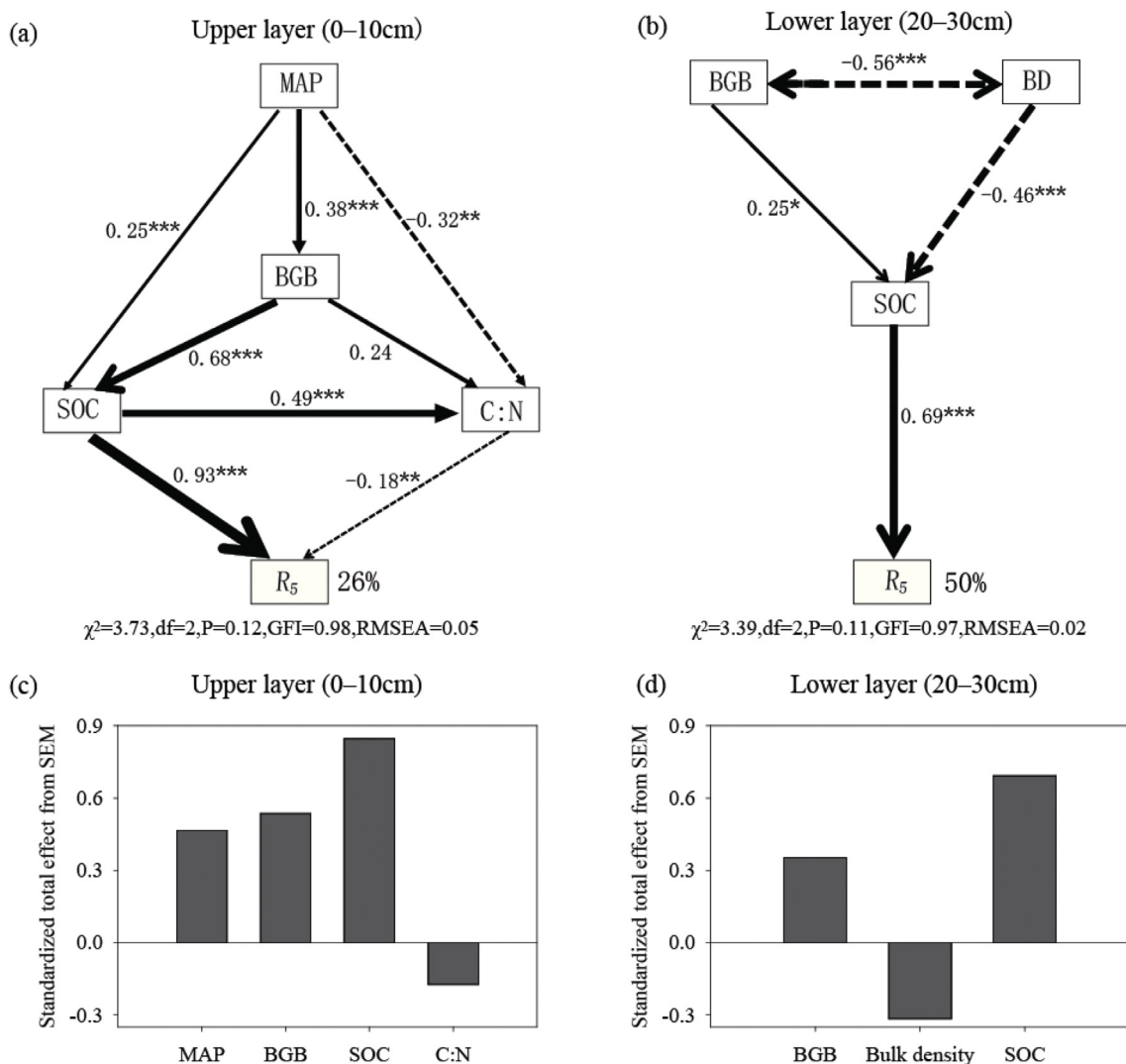


Fig. 5. Structural equation model (SEM) of factors regulating the spatial variation in SOC decomposition rate at 5 °C (R_5) in the upper (a) and lower (b) layers across Tibetan permafrost regions; standardized total effects on R_5 in the upper (c) and lower (d) layers. Numbers adjacent to arrows indicate the effect size of the relationship between the two variables. Solid and dashed arrows represent the positive and negative effects in the fitted structural equation model, respectively. Widths of the arrows indicate the strength of the casual relationship. MAP, BGB, and BD represent mean annual precipitation, belowground biomass, and bulk density, respectively. *, **, and *** represent $P < 0.05$, $P < 0.01$, and $P < 0.001$, respectively.

subsurface soil (10–30 cm), whereas C loss was found in surface soil (0–10 cm). This phenomenon is possible because C-turnover in the surface soil is easily affected by climatic changes (Mathieu et al., 2015), while in subsurface soil, the positive influences of climate warming and wetting on SOC turnover may be limited by a higher degree of protection of soil aggregates, SOC-mineral interactions (Salome et al., 2010), and more severe nutrient limitations (Fierer et al., 2003). In addition, Q_{10} value was higher in the lower than the upper layer, suggesting that soil C in the lower layer is currently more vulnerable to global warming. This pattern should be incorporated into soil C models to accurately evaluate the response of soil C to climate warming in permafrost regions.

4.2. Soil C content governed decomposition rate in both the upper and lower layers

SEM analyses revealed that SOC content was a main factor regulating the spatial variation in SOC decomposition rate in both the upper and lower soil layers across Tibetan permafrost regions (Fig. 5). By analysing 84 mineral soils from the US, Colman and Schimel (2013) also showed a positive relationship between microbial respiration and C

concentration. Higher SOC content is usually associated with a larger labile C pool (Colman and Schimel, 2013) and a greater soil enzyme activity (Hernández and Hobbie, 2010). Another important factor was BGB, which indirectly regulated the SOC decomposition rate in both layers via its positive effects on SOC content (Fig. S6).

In this study, MAP and C:N ratio indirectly affected SOC decomposition rate in the upper layer, whereas bulk density was significant only in the lower layer (Fig. 5). Across our study area, higher MAP led to greater BGB (Zhang et al., 2014), and hence a higher SOC content, but only in the upper layer (Fig. S7). Furthermore, higher MAP led to a lower soil C:N ratio (Fig. S8), possibly because increasing soil moisture increased the activity of microbial N fixation on the Tibetan Plateau (Kathrin et al., 2018). The lower soil C:N ratio is directly associated with higher SOC decomposition rates, as has been found across numerous studies (e.g., Zhang et al., 2008a; Wang et al., 2015; Xu et al., 2016). These effects were only significant in the upper layer, possibly because the ranges of soil C:N ratio and SOC content were larger than in the lower layer. SOC content was the only direct driver of the SOC decomposition rate in the lower layer (Fig. 5), demonstrating the connection between soil physical and biotic properties in regulating SOC decomposition (Rabbi et al., 2016). More direct evidence should be

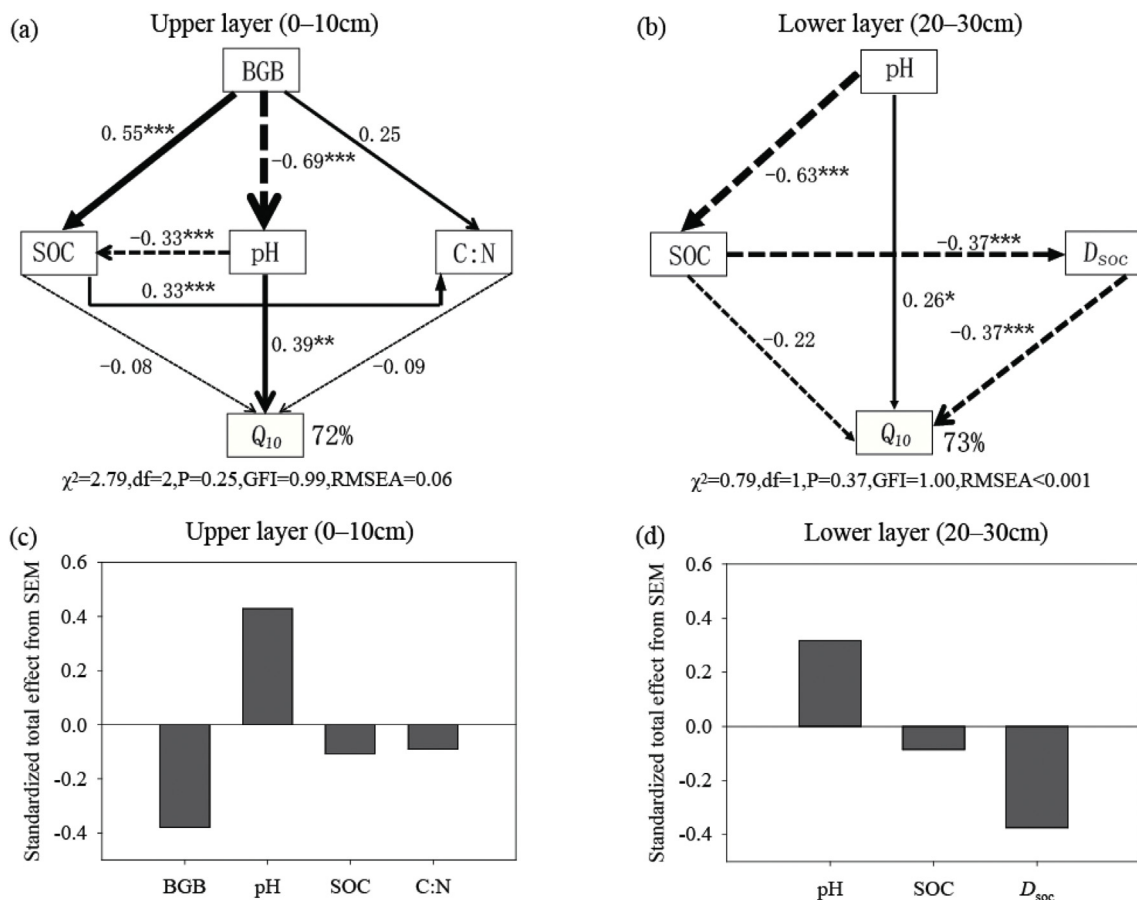


Fig. 6. Structural equation model (SEM) of factors regulating the temperature sensitivity of SOC decomposition (Q_{10}) in the upper (a) and lower (b) layers across Tibetan permafrost regions; standardized total effects on Q_{10} values in the upper (c) and lower (d) layers. Solid and dashed arrows represent the positive and negative effects in the fitted structural equation model, respectively. Widths of the arrows indicate the strength of the casual relationship. BGB and D_{soc} represent belowground biomass and SOC decomposability obtained from Eq. (4), respectively. *, **, and *** represent $P < 0.05$, $P < 0.01$, and $P < 0.001$, respectively.

obtained to further explore these results, such as how the effect of C:N ratio on microbial community activities varies with soil depth.

4.3. Contrasting depth-dependent determinants of Q_{10} value

Soil pH significantly and positively affected Q_{10} values in the upper layer across Tibetan permafrost regions (Fig. 6c). Craine et al. (2010) found that soil pH explained 67% of the variation in Q_{10} value across 71 grassland sites in North America. In 22 forest and 30 grassland sites across China, Liu et al. (2017) also found that pH explained 42% of the regional variation in Q_{10} values. Such a relationship could be explained by the effects of soil pH on microbial community composition (Bååth and Anderson, 2003). Soil microbial community composition is often denoted by the fungal-to-bacterial ratio, which increases with increasing soil pH (Bååth and Anderson, 2003). High fungal-to-bacterial ratios are associated with greater temperature sensitivity of SOC decomposition (Briones et al., 2014), leading to increased Q_{10} value with increasing soil pH. In addition, BGB indirectly affected Q_{10} values via its negative relationship with soil pH across Tibetan permafrost regions (Fig. 6a), which was not found in previous non-permafrost studies. One possible explanation is that higher BGB would lead to greater deposition of organic acids within the rhizosphere (Valentinuzzi et al., 2015), resulting in lower pH.

In contrast to the upper layer, SOC decomposability played the most important role in mediating the spatial variation in Q_{10} values in the lower layer across Tibetan permafrost regions (Fig. 6c). As mentioned above, similarly to the parameter B from Eq. (1) in previous studies (e.g., Fierer et al., 2006; Ding et al., 2016a), we used D_{soc} as an index of

SOC decomposability (availability and lability) of the substrates. A negative relationship between Q_{10} value and D_{soc} was found in the lower layer, demonstrating that C with higher decomposability has a lower Q_{10} value, thereby supporting the CQT hypothesis (Bosatta and Ågren, 1999; Davidson and Janssens, 2006).

4.4. Possible effects of CO_2 measurement methods on Q_{10} estimation

By definition, Q_{10} is the change in SOC decomposition rate with temperature under otherwise constant conditions (Davidson and Janssens, 2006). Soil incubations are usually used to estimate the inherent sensitivity of soil C to warming (e.g., Fierer et al., 2006; Craine et al., 2010; Ding et al., 2016a). Generally, there are two types of soil incubation methods for Q_{10} value estimation (i.e., parallel and sequential incubation approaches) (Li et al., 2017). The sequential method has been often used, especially to compare Q_{10} values across a wide variety of soils (Ding et al., 2016a; Liu et al., 2017).

Surprisingly, a recent study in the same area by Ding et al. (2016a), involving 156 sites across the alpine grasslands, showed that the mean soil respiration rate at 5 °C (R_5) was $0.05 \mu g CO_2-C g^{-1} soil h^{-1}$ and that Q_{10} value was 4.29 at 0–10 cm soil depth. Compared with the findings of Ding et al. (2016a), our results for R_5 were approximately 180% higher, but the Q_{10} value was approximately 34% lower. Our continuous-flow incubation system allowed all jars to be incubated simultaneously for the same amount of time and minimized the dissolution of CO_2 in the water phase of the samples for alkaline soils (the mean pH was 8.04 in 0–10 cm soil depth across the alpine grasslands in this study). In contrast, the standard method uses decreasing incubation

time with increasing incubation temperature, varying from several hours to days at high and low temperatures, respectively (e.g., Leifeld and Fuhrer, 2005; Ding et al., 2016a). This may underestimate the respiration rate, especially at low temperatures, and consequently overestimate Q_{10} value, because longer incubation time might allow for greater CO_2 dissolution in the water phase. Therefore, we suggest that the continuous-flow incubation approach is advantageous for measuring SOC decomposition rate and its temperature sensitivity, especially for alkaline soils.

5. Conclusions

Our results suggest that the subsurface soil C is more vulnerable to loss with increasing temperature across Tibetan permafrost regions. Previous predictions of the strength of the C-climate feedbacks in permafrost regions may be underestimated because many soil C models treat the whole soil profile as a homogeneous unit (e.g., Koven et al., 2015) and ignore the higher temperature sensitivity of subsurface soil C to warming. The differences in SOC decomposition rate and Q_{10} values as well as their controlling factors between the two soil layers should be incorporated into soil C models to produce reliable projections of the future dynamics of permafrost C under a warming climate.

Acknowledgements

This work was supported by the National Key Research and Development Program of China (2017YFC1200100 and 2018YFC1406402), the National Science Foundation of China (41630528 and 31670491), the Young Thousand Talents Program Scholar, the Shanghai Pujiang Scholar Program (16PJ1400900), and E.P. acknowledges support from Australian Research Council grant DP170102766. J.L. acknowledges the financial support from China Scholarship Council (CSC).

Appendix A. Supplementary data

Supplementary data related to this chapter can be found at <https://doi.org/10.1016/j.soilbio.2018.08.015>.

Declarations of conflict of interest

None.

References

- Bååth, E., Anderson, T.H., 2003. Comparison of soil fungal/bacterial ratios in a pH gradient using physiological and PLFA-based techniques. *Soil Biology and Biochemistry* 35, 955–963.
- Balesdent, J., Basile-Doelsch, I., Chadoeuf, J., Cornu, S., Derrien, D., Fekiacova, Z., Hatté, C., 2018. Atmosphere–soil carbon transfer as a function of soil depth. *Nature* 599, 599–602.
- Bosatta, E., Ågren, G.I., 1999. Soil organic matter quality interpreted thermodynamically. *Soil Biology and Biochemistry* 31, 1889–1891.
- Briones, M.J.I., McNamara, N.P., Poskitt, J., Crow, S.E., Ostle, N.J., 2014. Interactive biotic and abiotic regulators of soil carbon cycling: evidence from controlled climate experiments on peatland and boreal soils. *Global Change Biology* 20, 2971–2982.
- Chen, L., Flynn, D.F.B., Jing, X., Kühn, P., Scholten, T., He, J.-S., 2015. A comparison of two methods for quantifying soil organic carbon of alpine grasslands on the Tibetan Plateau. *PLoS One* 10, e0126372.
- Chen, Y., Ding, J., Peng, Y., Li, F., Yang, G., Liu, L., Qin, S., Fang, K., Yang, Y., 2016. Patterns and drivers of soil microbial communities in Tibetan alpine and global terrestrial ecosystems. *Journal of Biogeography* 43, 2027–2039.
- Chinese Academy of Sciences, 2001. *Vegetation Atlas of China*. Science Press, Beijing.
- Colman, B.P., Schimel, J.P., 2013. Drivers of microbial respiration and net N mineralization at the continental scale. *Soil Biology and Biochemistry* 60, 65–76.
- Craine, J., Spurr, R., McLauchlan, K., Fierer, N., 2010. Landscape-level variation in temperature sensitivity of soil organic carbon decomposition. *Soil Biology and Biochemistry* 42, 373–375.
- Davidson, E.A., Janssens, I.A., 2006. Temperature sensitivity of soil carbon decomposition and feedbacks to climate change. *Nature* 440, 165–173.
- Ding, J., Chen, L., Ji, C., Hugelius, G., Li, Y., Liu, L., Qin, S., Zhang, B., Yang, G., Li, F., Fang, K., Chen, Y., Peng, Y., Zhao, X., He, H., Smith, P., Fang, J., Yang, Y., 2017. Decadal soil carbon accumulation across Tibetan permafrost regions. *Nature Geoscience* 10, 420–424.
- Ding, J., Chen, L., Zhang, B., Liu, L., Yang, G., Fang, K., Chen, Y., Li, F., Kou, D., Ji, C., Luo, Y., Yang, Y., 2016a. Linking temperature sensitivity of soil CO_2 release to substrate, environmental, and microbial properties across alpine ecosystems. *Global Biogeochemical Cycles* 30, 1310–1323.
- Ding, J., Li, F., Yang, G., Chen, L., Zhang, B., Liu, L., Fang, K., Qin, S., Chen, Y., Peng, Y., Ji, C., He, H., Smith, P., Yang, Y., 2016b. The permafrost carbon inventory on the Tibetan Plateau: a new evaluation using deep sediment cores. *Global Change Biology* 22, 2688–2701.
- Fierer, N., Allen, A.S., Schimel, J.P., Holden, P.A., 2003. Controls on microbial CO_2 production: a comparison of surface and subsurface soil horizons. *Global Change Biology* 9, 1322–1332.
- Fierer, N., Colman, B.P., Schimel, J.P., Jackson, R.B., 2006. Predicting the temperature dependence of microbial respiration in soil: a continental-scale analysis. *Global Biogeochemical Cycles* 20, GB3026.
- Hassink, J., Whitmore, A.P., 1997. A model of the physical protection of organic matter in soils. *Soil Science Society of America Journal* 61, 131–139.
- Hernández, D.L., Hobbie, S.E., 2010. The effects of substrate composition, quantity, and diversity on microbial activity. *Plant and Soil* 335, 397–411.
- Hicks Pries, C.E., Castanha, C., Porras, R.C., Torn, M.S., 2017. The whole-soil carbon flux in response to warming. *Science* 355, 1420–1423.
- IPCC, 2013. Annex I: atlas of global and regional climate projections. van Oldenborgh, G.J., M. Collins, J. Arblaster, J.H. Christensen, J. Marotzke, S.B. Power, M. Rummukainen and T. Zhou In: Stocker, T.F., Qin, D., Plattner, G.-K., Tignor, M., Allen, S.K., Boschung, J., Nauels, A., Xia, Y., Bex, V., Midgley, P.M. (Eds.), *Climate Change 2013: the Physical Science Basis. Contribution of Working Group I to the Fifth Assessment Report of the Intergovernmental Panel on Climate Change*. Cambridge University Press, Cambridge, United Kingdom and New York, NY, USA.
- Jia, J., Feng, X., He, J.-S., He, H., Lin, L., Liu, Z., 2017. Comparing microbial carbon sequestration and priming in the subsoil versus topsoil of a Qinghai-Tibetan alpine grassland. *Soil Biology and Biochemistry* 104, 141–151.
- Jobby, E.G., Jackson, R.B., 2000. The vertical distribution of soil organic carbon and its relation to climate and vegetation. *Ecological Applications* 10, 423–436.
- Kathrin, R., Laerkedal, S.P., Anders, M., 2018. What drives biological nitrogen fixation in high arctic tundra: moisture or temperature? *Ecosphere* 9, e02117.
- Koven, C.D., Lawrence, D.M., Riley, W.J., 2015. Permafrost carbon-climate feedback is sensitive to deep soil carbon decomposability but not deep soil nitrogen dynamics. *Proceedings of the National Academy of Sciences* 112, 3752–3757.
- Leifeld, J., Fuhrer, J., 2005. The temperature response of CO_2 production from bulk soils and soil fractions is related to soil organic matter quality. *Biogeochemistry* 75, 433–453.
- Li, J.Q., Pei, J.M., Cui, J., Chen, X.P., Li, B., Nie, M., Fang, C.M., 2017. Carbon quality mediates the temperature sensitivity of soil organic carbon decomposition in managed ecosystems. *Agriculture, Ecosystems & Environment* 250, 44–50.
- Li, L., Yang, S., Wang, Z.Y., Zhu, X.D., Tang, H.Y., 2010. Evidence of warming and wetting climate over the Qinghai-Tibet Plateau. *Arctic Antarctic and Alpine Research* 42, 449–457.
- Li, W., Zhou, X., 1998. *Ecosystems of Qinghai-Xizang (Tibetan) Plateau and Approach for Their Sustainable Management*. Guangdong Science & Technology Press, Guangzhou.
- Liu, W., Chen, S., Qin, X., Baumann, F., Scholten, T., Zhou, Z., Sun, W., Zhang, T., Ren, J., Qin, D., 2012. Storage, patterns, and control of soil organic carbon and nitrogen in the northeastern margin of the Qinghai-Tibetan Plateau. *Environmental Research Letters* 7, 035401.
- Liu, Y., He, N., Zhu, J., Xu, L., Yu, G., Niu, S., Sun, X., Wen, X., 2017. Regional variation in the temperature sensitivity of soil organic matter decomposition in China's forests and grasslands. *Global Change Biology* 23, 3393–3402.
- Mathieu, J., Christine, H., Balesdent, J., Parent, É., 2015. Deep soil carbon dynamics are driven more by soil type than by climate: a worldwide meta-analysis of radiocarbon profiles. *Global Change Biology* 21, 4278–4292.
- Mu, C., Zhang, T., Wu, Q., Peng, X., Cao, B., Zhang, X., Cao, B., Cheng, G., 2015. Editorial: organic carbon pools in permafrost regions on the Qinghai-Xizang (Tibetan) Plateau. *The Cryosphere* 9, 479–486.
- Pang, Q., Cheng, G., Li, S., Zhang, W., 2009. Active layer thickness calculation over the Qinghai-Tibet Plateau. *Cold Regions Science and Technology* 57, 23–28.
- Rabbi, S.M.F., Daniel, H., Lockwood, P.V., Macdonald, C., Pereg, L., Tighe, M., Wilson, B.R., Young, I.M., 2016. Physical soil architectural traits are functionally linked to carbon decomposition and bacterial diversity. *Scientific Reports* 6, 33012.
- Rodionov, A., Flessa, H., Kazansky, O., Guggenberger, G., 2006. Organic matter composition and potential trace gas production of permafrost soils in the forest tundra in northern Siberia. *Geoderma* 135, 49–62.
- Salome, C., Nunan, N., Pouteau, V., Lerch, T.Z., Chenu, C., 2010. Carbon dynamics in topsoil and in subsoil may be controlled by different regulatory mechanisms. *Global Change Biology* 16, 416–426.
- Schädel, C., Bader, M.K.F., Schuur, E.A.G., Biasi, C., Bracho, R., Čapek, P., De Baets, S., Diáková, K., Ernakovich, J., Estop-Aragones, C., Graham, D.E., Hartley, I.P., Iversen, C.M., Kane, E., Knoblauch, C., Lupascu, M., Martikainen, P.J., Natali, S.M., Norby, R.J., O'Donnell, Jonathan A., Chowdhury, T.R., Šantrůčková, H., Shaver, G., Sloan, Victoria L., Treat, C.C., Turetsky, M.R., Waldrop, M.P., Wickland, K.P., 2016. Potential carbon emissions dominated by carbon dioxide from thawed permafrost soils. *Nature Climate Change* 6, 950–953.
- Schädel, C., Schuur, E.A.G., Bracho, R., Elberling, B., Knoblauch, C., Lee, H., Luo, Y., Shaver, G.R., Turetsky, M.R., 2014. Circumpolar assessment of permafrost C quality and its vulnerability over time using long-term incubation data. *Global Change Biology* 20, 641–652.
- Schuur, E.A.G., Bockheim, J., Canadell, J.G., Euskirchen, E., Field, C.B., Goryachkin, S.V.,

- Hagemann, S., Kuhry, P., Lafleur, P.M., Lee, H., Mazhitova, G., Nelson, F.E., Rinke, A., Romanovsky, V.E., Shiklomanov, N., Tarnocai, C., Venevsky, S., Vogel, J.G., Zimov, S.A., 2008. Vulnerability of permafrost carbon to climate change: implications for the global carbon cycle. *BioScience* 58, 701–714.
- Schuur, E.A.G., McGuire, A.D., Schädel, C., Grosse, G., Harden, J.W., Hayes, D.J., Hugelius, G., Koven, C.D., Kuhry, P., Lawrence, D.M., Natali, S.M., Olefeldt, D., Romanovsky, V.E., Schaefer, K., Turetsky, M.R., Treat, C.C., Vonk, J.E., 2015. Climate change and the permafrost carbon feedback. *Nature* 520, 171–179.
- Tarnocai, C., Canadell, J.G., Schuur, E.A.G., Kuhry, P., Mazhitova, G., Zimov, S., 2009. Soil organic carbon pools in the northern circumpolar permafrost region. *Global Biogeochemical Cycles* 23, GB2023.
- Valentinuzzi, F., Mimmo, T., Cesco, S., Al Mamun, S., Santner, J., Hoefler, C., Oburger, E., Robinson, B., Lehto, N., 2015. The effect of lime on the rhizosphere processes and elemental uptake of white lupin. *Environmental and Experimental Botany* 118, 85–94.
- Waldrop, M.P., Wickland, K.P., White III, R., Berhe, A.A., Harden, J.W., Romanovsky, V.E., 2010. Molecular investigations into a globally important carbon pool: permafrost-protected carbon in Alaskan soils. *Global Change Biology* 16, 2543–2554.
- Wang, B., Bao, Q., Hoskins, B., Wu, G., Liu, Y., 2008. Tibetan Plateau warming and precipitation changes in East Asia. *Geophysical Research Letters* 35, L14702.
- Wang, B., French, H.M., 1995. Permafrost on the Tibet Plateau, China. *Quaternary Science Reviews* 14, 255–274.
- Wang, J., Wang, X., Xu, M., Feng, G., Zhang, W., Yang, X., Huang, S., 2015. Contributions of wheat and maize residues to soil organic carbon under long-term rotation in north China. *Scientific Reports* 5, 11409.
- Wang, X., Song, C., Wang, J., Miao, Y., Mao, R., Song, Y., 2013. Carbon release from *Sphagnum* peat during thawing in a montane area in China. *Atmospheric Environment* 75, 77–82.
- Wu, Q., Zhang, T., 2008. Recent permafrost warming on the Qinghai-Tibetan Plateau. *Journal of Geophysical Research: Atmospheres* 113, D13108.
- Xu, X., Shi, Z., Li, D., Rey, A., Ruan, H., Craine, J.M., Liang, J., Zhou, J., Luo, Y., 2016. Soil properties control decomposition of soil organic carbon: results from data-assimilation analysis. *Geoderma* 262, 235–242.
- You, Q., Kang, S., Pepin, N., Flügel, W.-A., Yan, Y., Behrawan, H., Huang, J., 2010. Relationship between temperature trend magnitude, elevation and mean temperature in the Tibetan Plateau from homogenized surface stations and reanalysis data. *Global and Planetary Change* 71, 124–133.
- Zhang, D., Hui, D., Luo, Y., Zhou, G., 2008a. Rates of litter decomposition in terrestrial ecosystems: global patterns and controlling factors. *Journal of Plant Ecology* 1, 85–93.
- Zhang, T., Barry, R.G., Knowles, K., Heginbottom, J.A., Brown, J., 2008b. Statistics and characteristics of permafrost and ground-ice distribution in the Northern Hemisphere. *Polar Geography* 31, 47–68.
- Zhang, Y., Qi, W., Zhou, C., Ding, M., Liu, L., Gao, J., Bai, W., Wang, Z., Zheng, D., 2014. Spatial and temporal variability in the net primary production of alpine grassland on the Tibetan Plateau since 1982. *Journal of Geographical Sciences* 24, 269–287.
- Zhou, T., Shi, P., Hui, D., Luo, Y., 2009. Global pattern of temperature sensitivity of soil heterotrophic respiration (Q_{10}) and its implications for carbon-climate feedback. *Journal of Geophysical Research: Biogeosciences* 114, G02016.
- Zhu, X., Wang, W., Fraedrich, K., 2013. Future climate in the Tibetan Plateau from a statistical regional climate model. *Journal of Climate* 26, 10125–10138.